

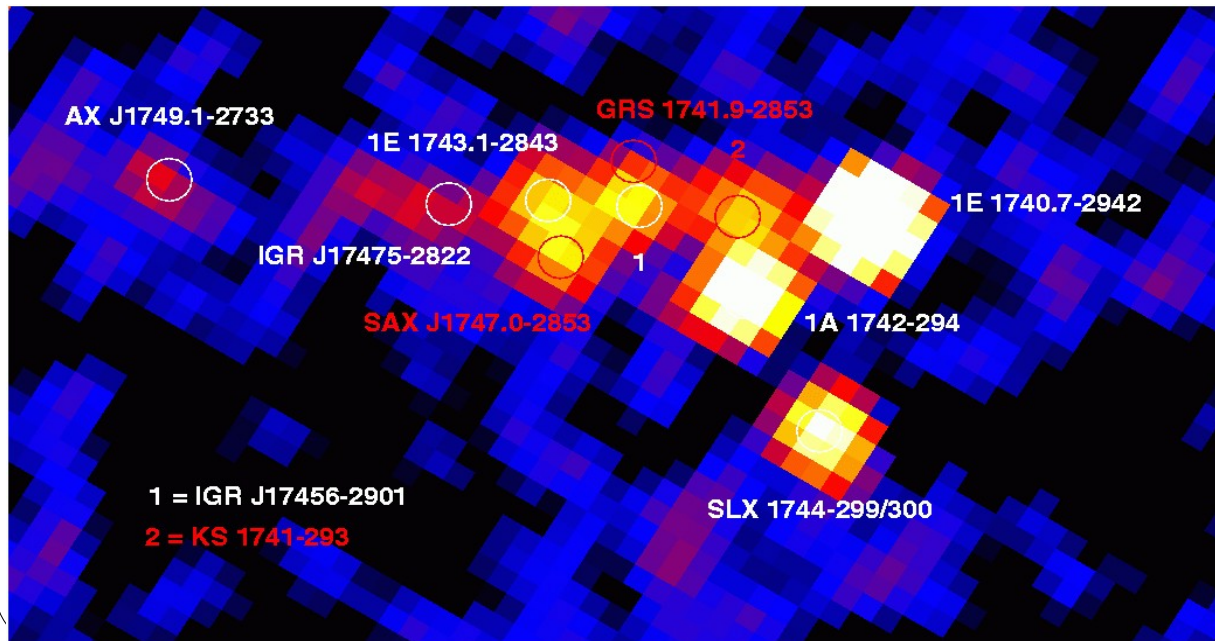
A “synthetic” view of AGN

- few words on activity in the central kpc of our Galaxy observed by INTEGRAL
- comprehensive view of 3C 273
- some ideas on shocks in the potential well of supermassive black holes.

Galactic centre

one image every 3 day
February 2005 to April 2006

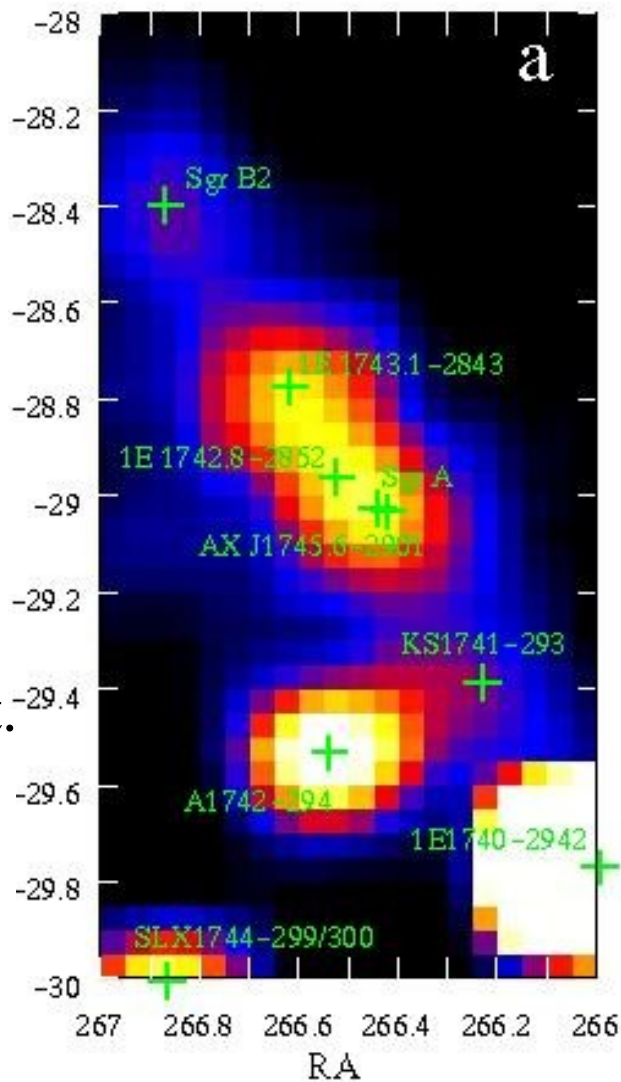
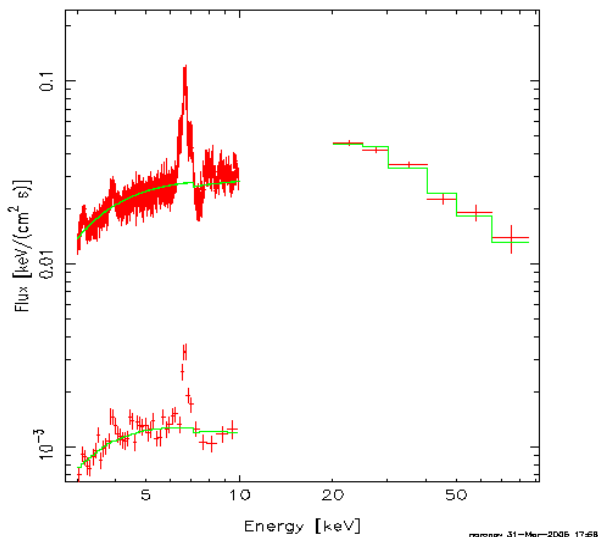
(February-April and August-October)



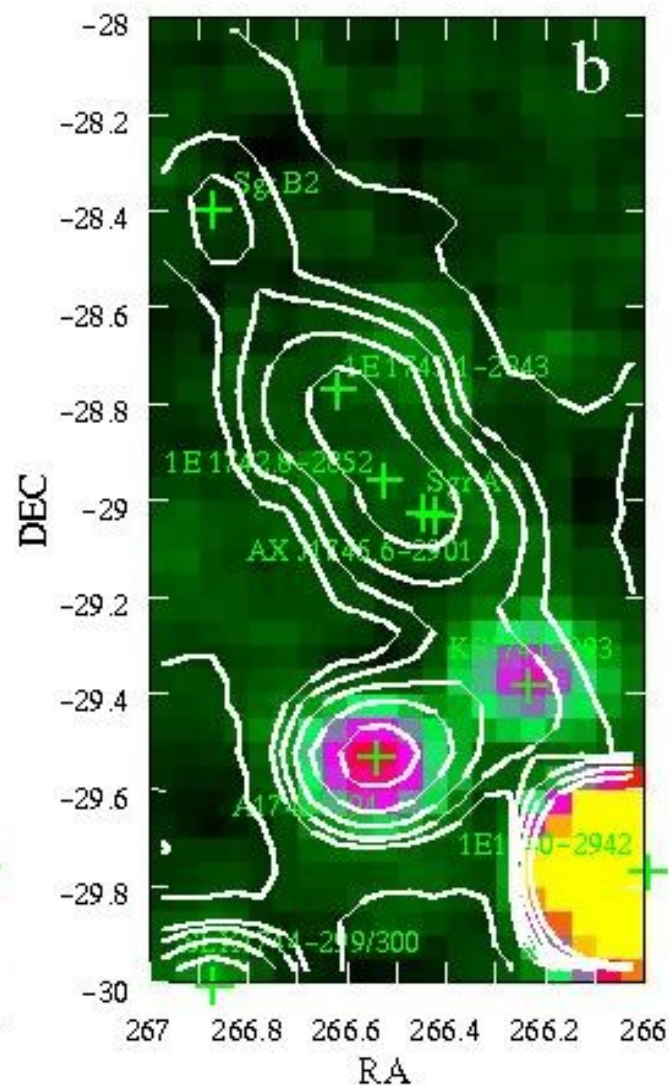
Averaged image

Variability of galactic centre less than 8%

Extended emission synchrotron,
 $B \sim .1 \text{ mG}$, $E \sim .1 \text{ PeV}$
 TeV flux: inv. Compt.

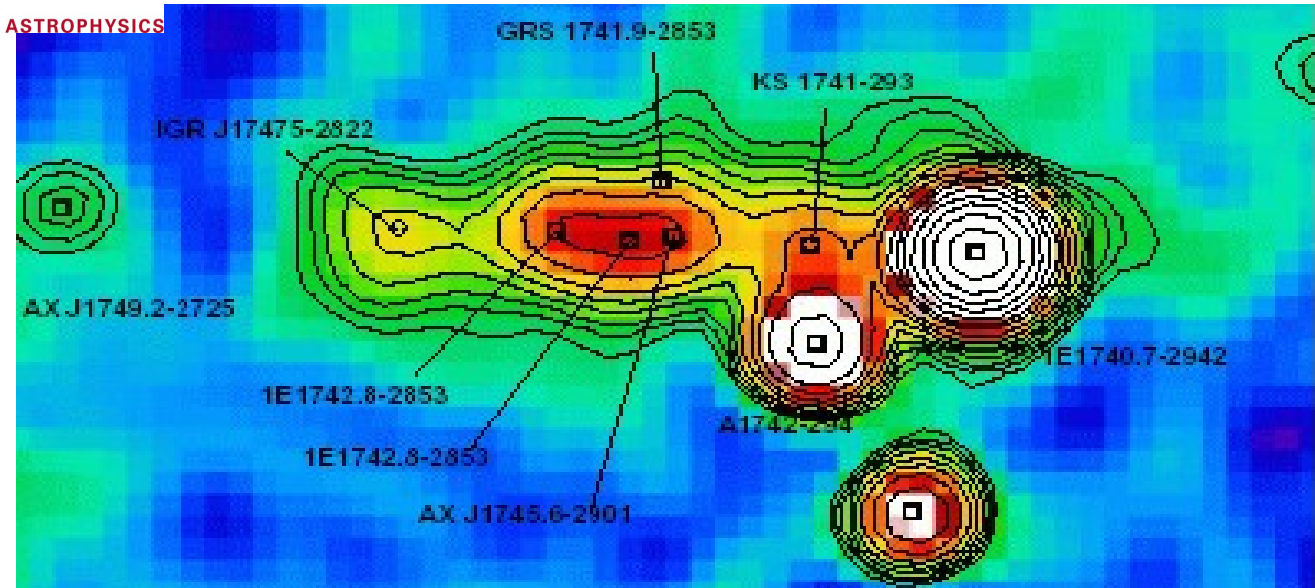


20-60keV
 Neronov et al. 2005

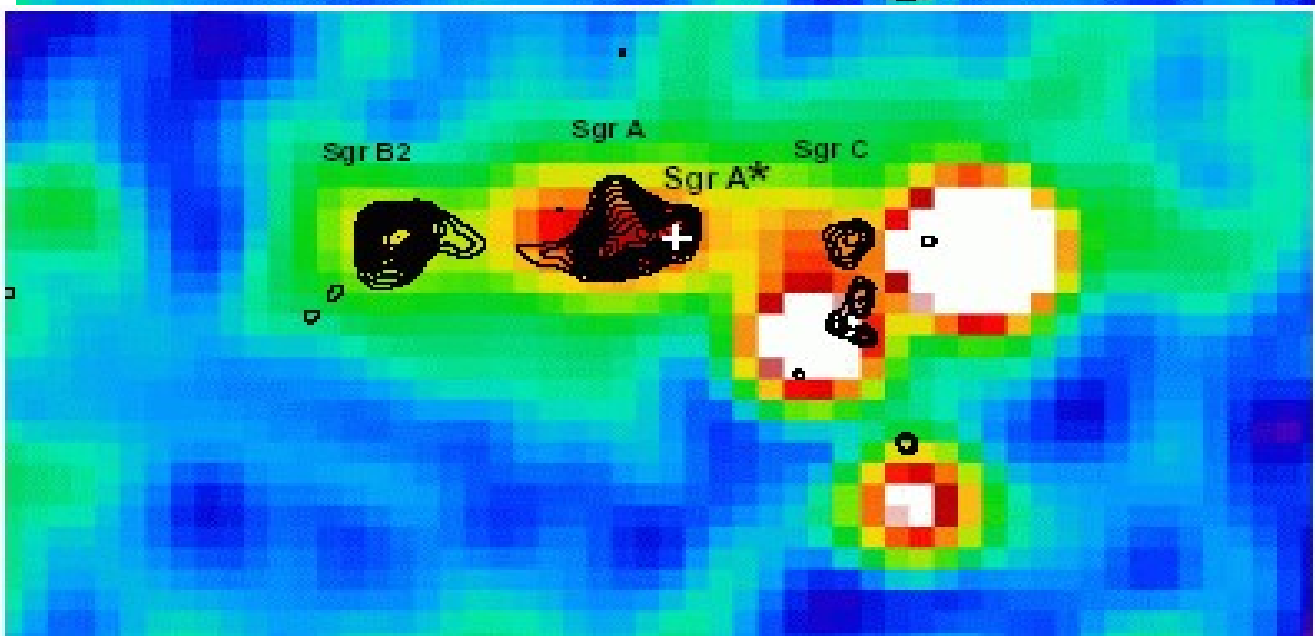


variability map

Galactic centre (Revnivtsev et al. 2004, A&A 425, L49)



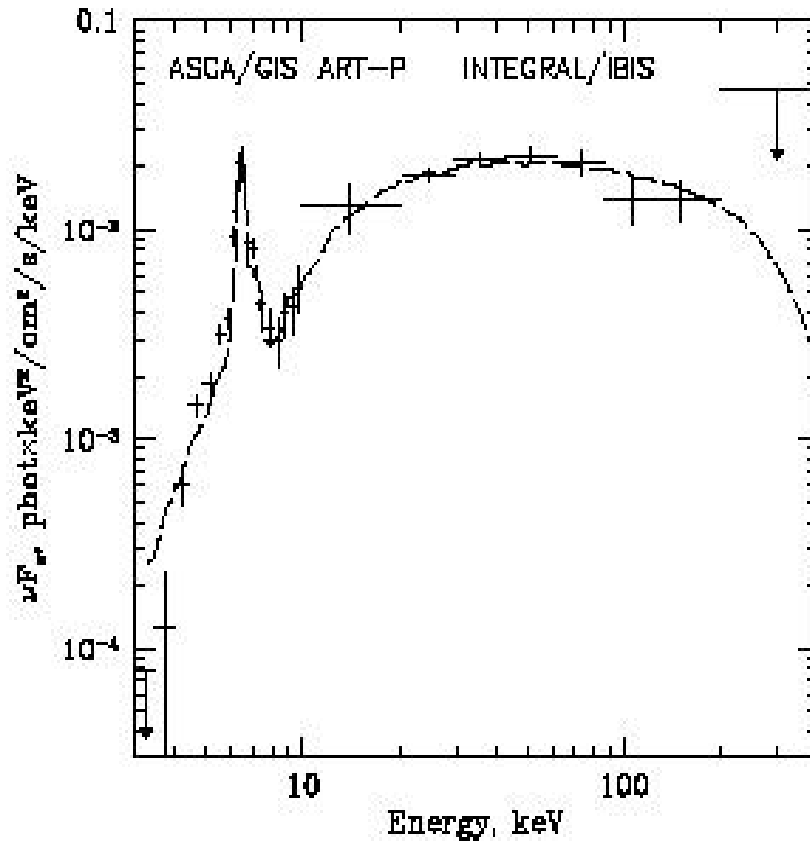
16-60keV
ISGRI data



Fe contours
ASCA
overplot

Galactic centre

(Revnivtsev et al. 2004, A&A 425, L49)



Broad band spectrum of
IGR 17475-2822

Typical of a reflection
component.

Reflection of SgrA*
at $5 \cdot 10^{38}$ ergs/s some
300 years ago

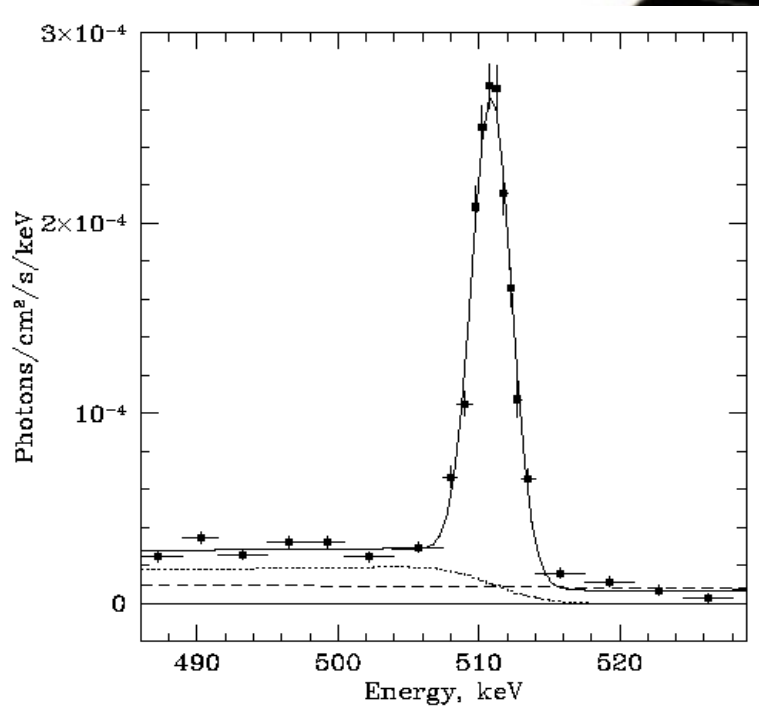
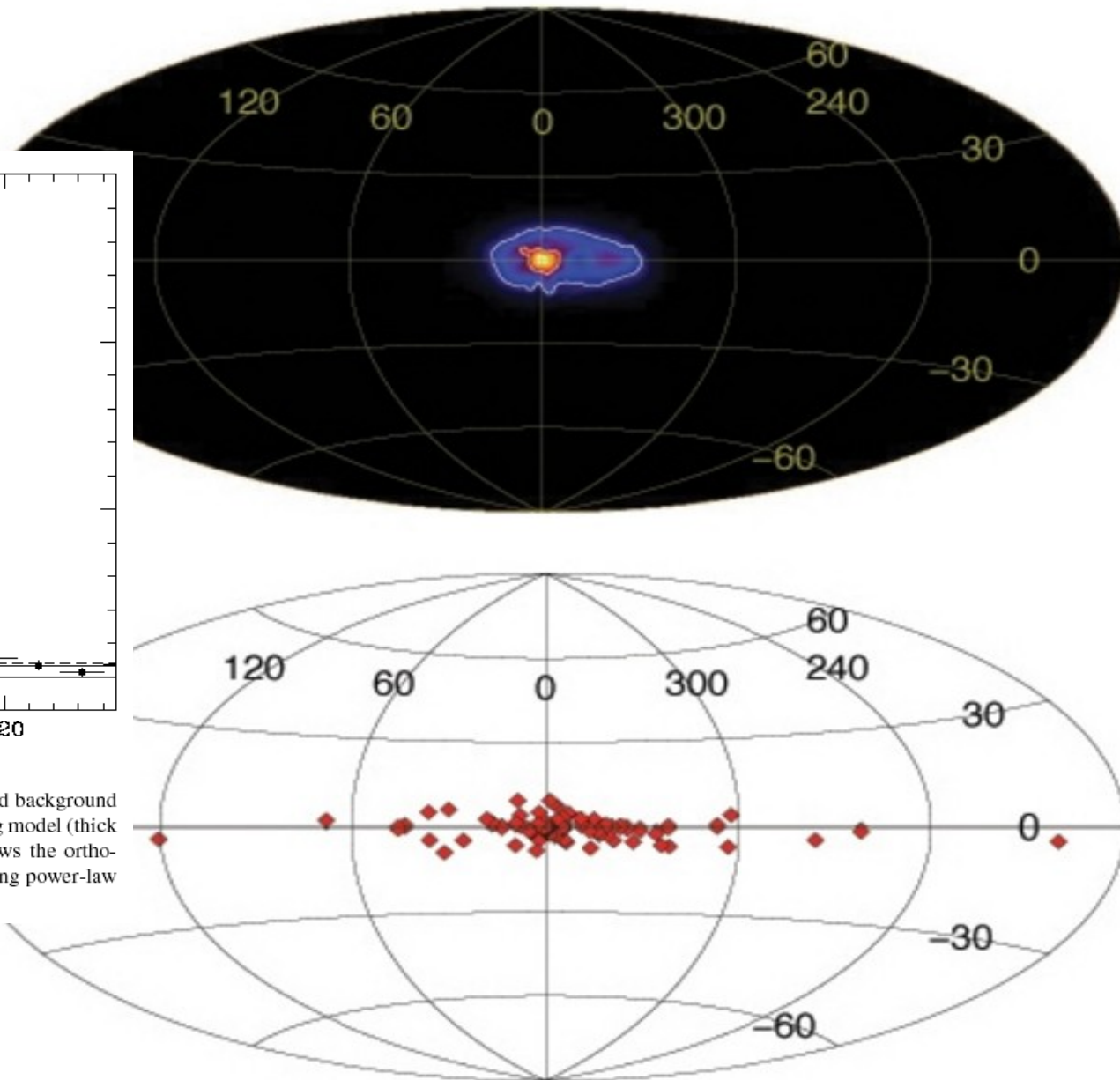
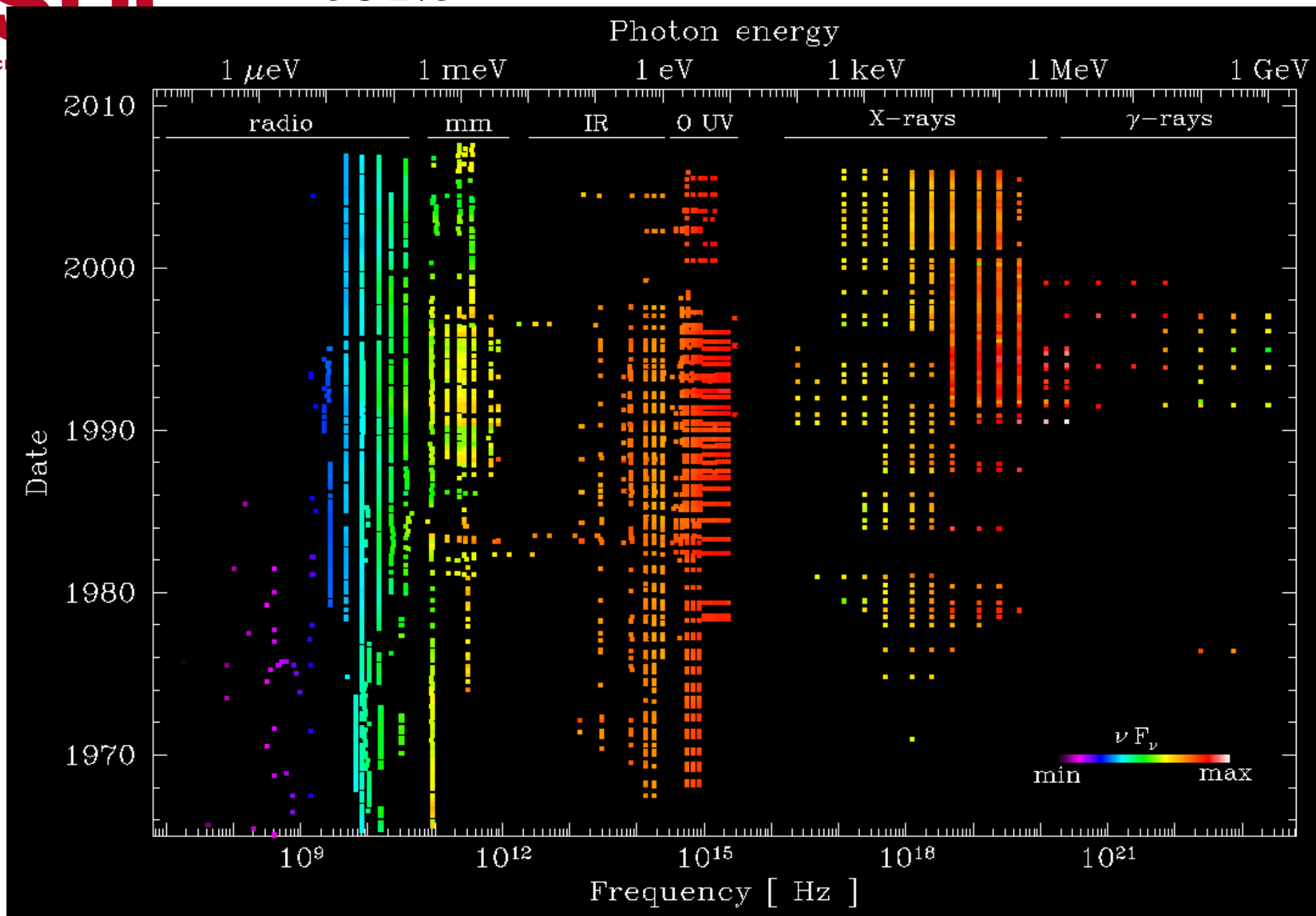


Figure 1. Spectrum of the e^+e^- annihilation radiation (fixed background model) detected by SPI from the GC region and the best-fitting model (thick solid line, see Table 1 for parameters). The dotted line shows the ortho-positronium radiation and the dashed line shows the underlying power-law continuum.

10^{43} annihilations/s
warm medium

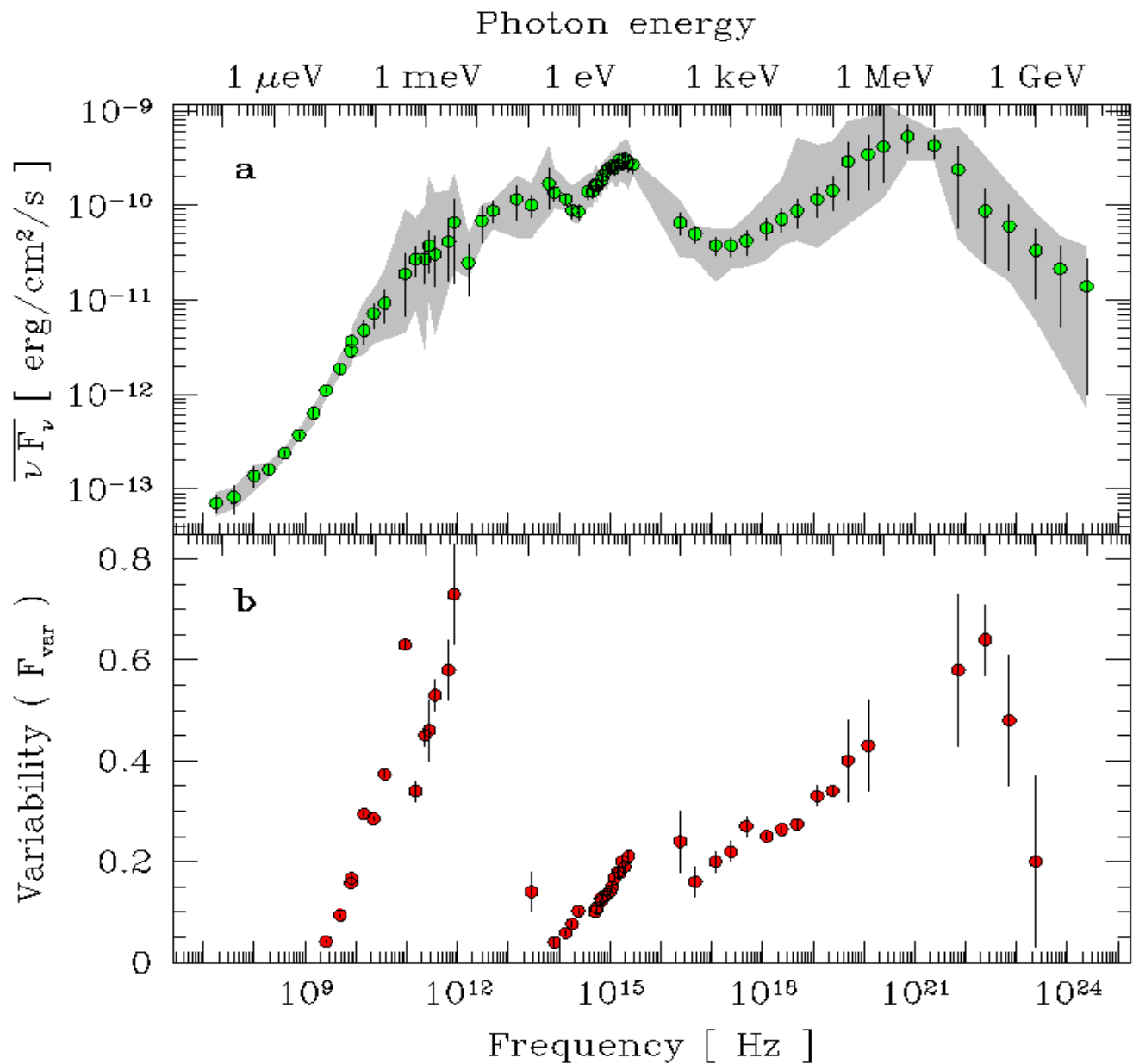
origin of positrons in LMXRB? Weidenspointner et al. 2008



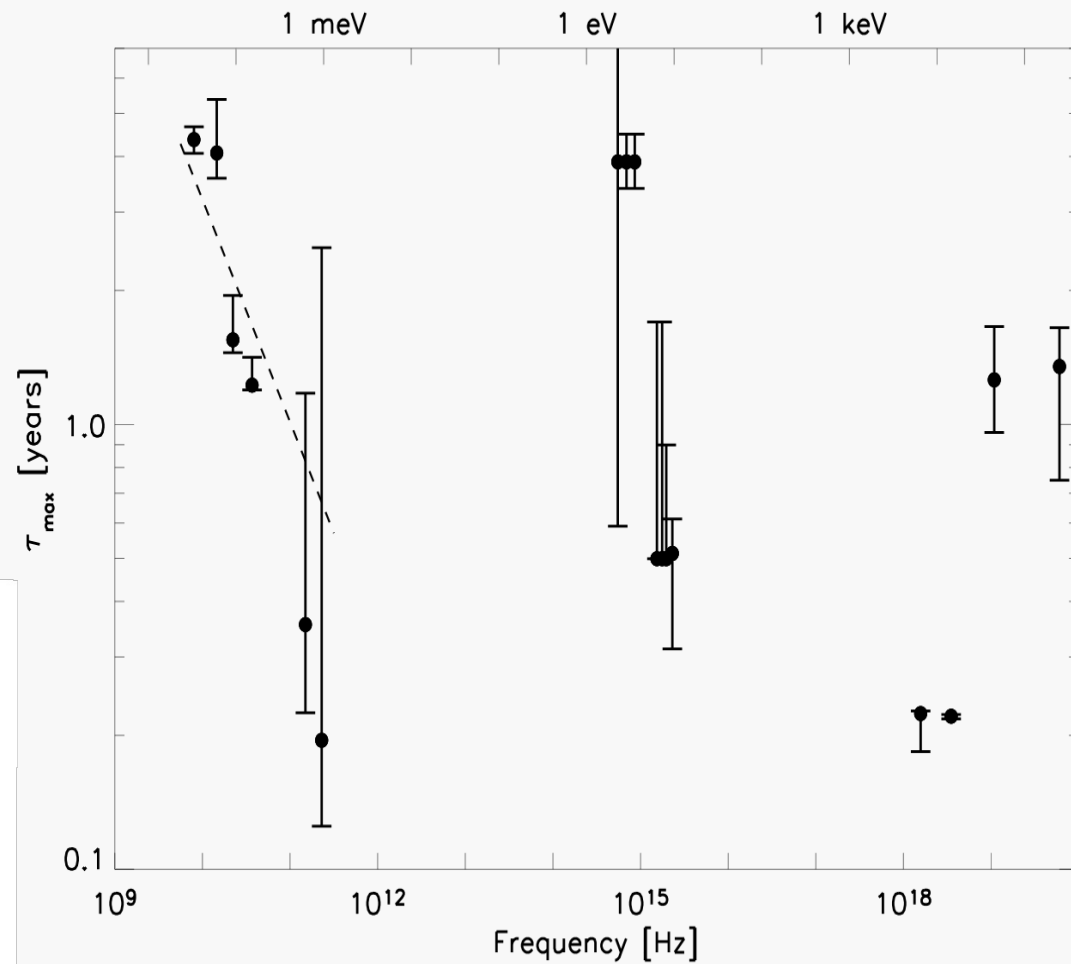
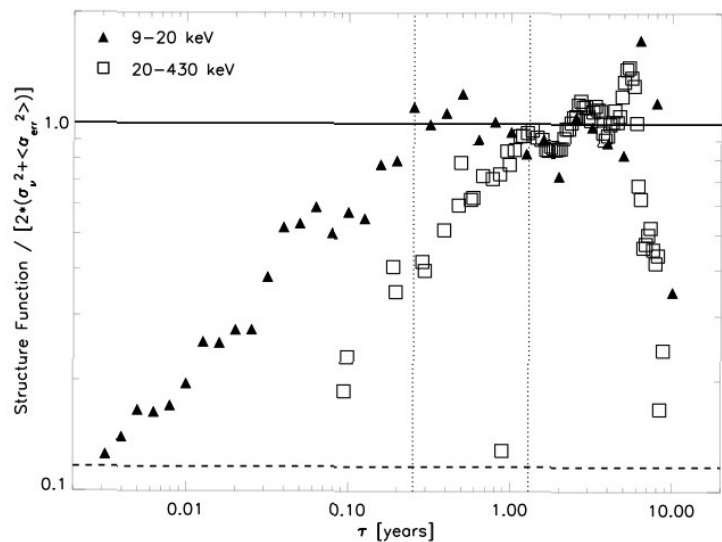


Average spectrum
and range of obs.
Fluxes

fractional variability



Maximum timescale observed as a function of photon energy



In the X-rays:

- 2-20keV flux varies with less amplitude than 20-100keV flux
20% and 40%

-2-20keV flux varies on shorter timescales than the harder X-rays
maximum variability time is 0.2yr and 1yr resp.

Either 2 components, the harder varying more and slower than the
softer

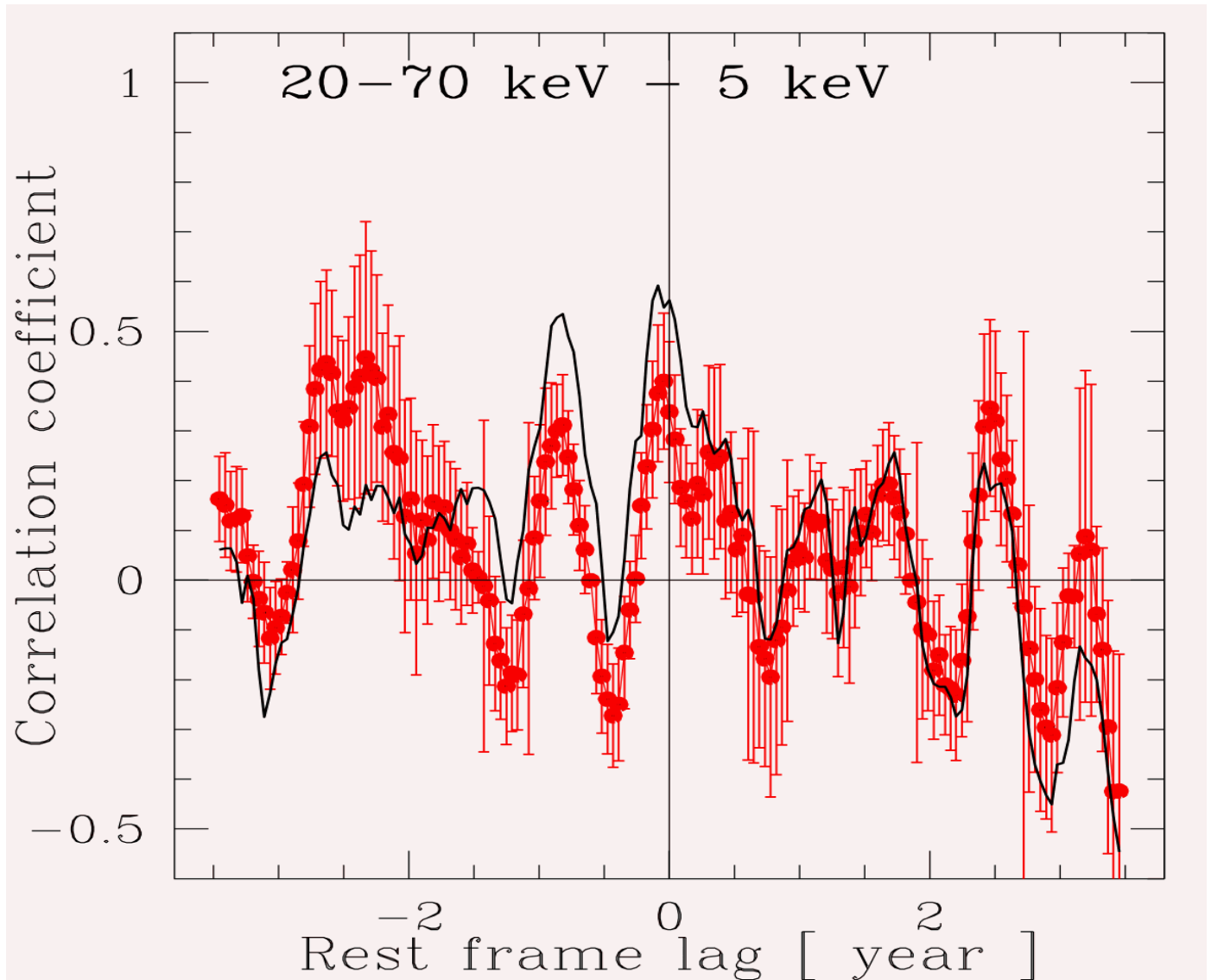
or slope and amplitude vary such that low energy normalisation
varies faster than (large) slow slope variations.

Cross correlation

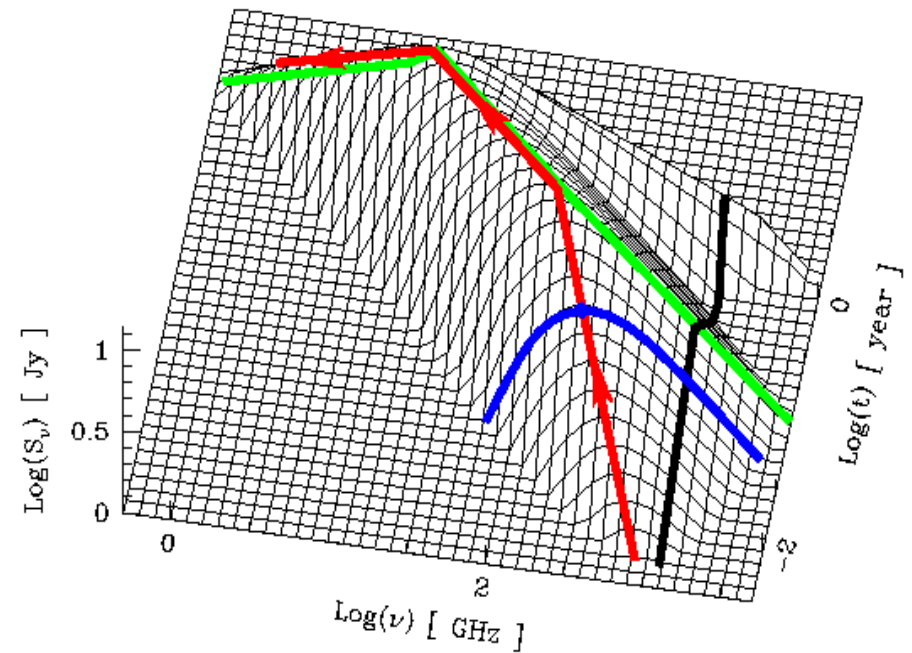
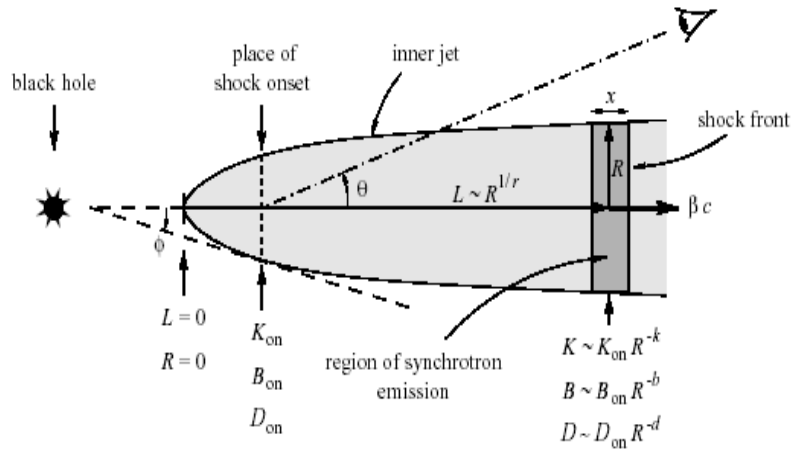
no correlation
between hard and
medium E X-rays

(range: bootstrap)
red: discrete method

i.e. Two components
are uncorrelated
or
slope and amplitude
var. uncorr.



3C 273 Jet modeling: Tuerler et al. 1999, 2000



Understand all the light curves from radio to far IR as a superposition of flares

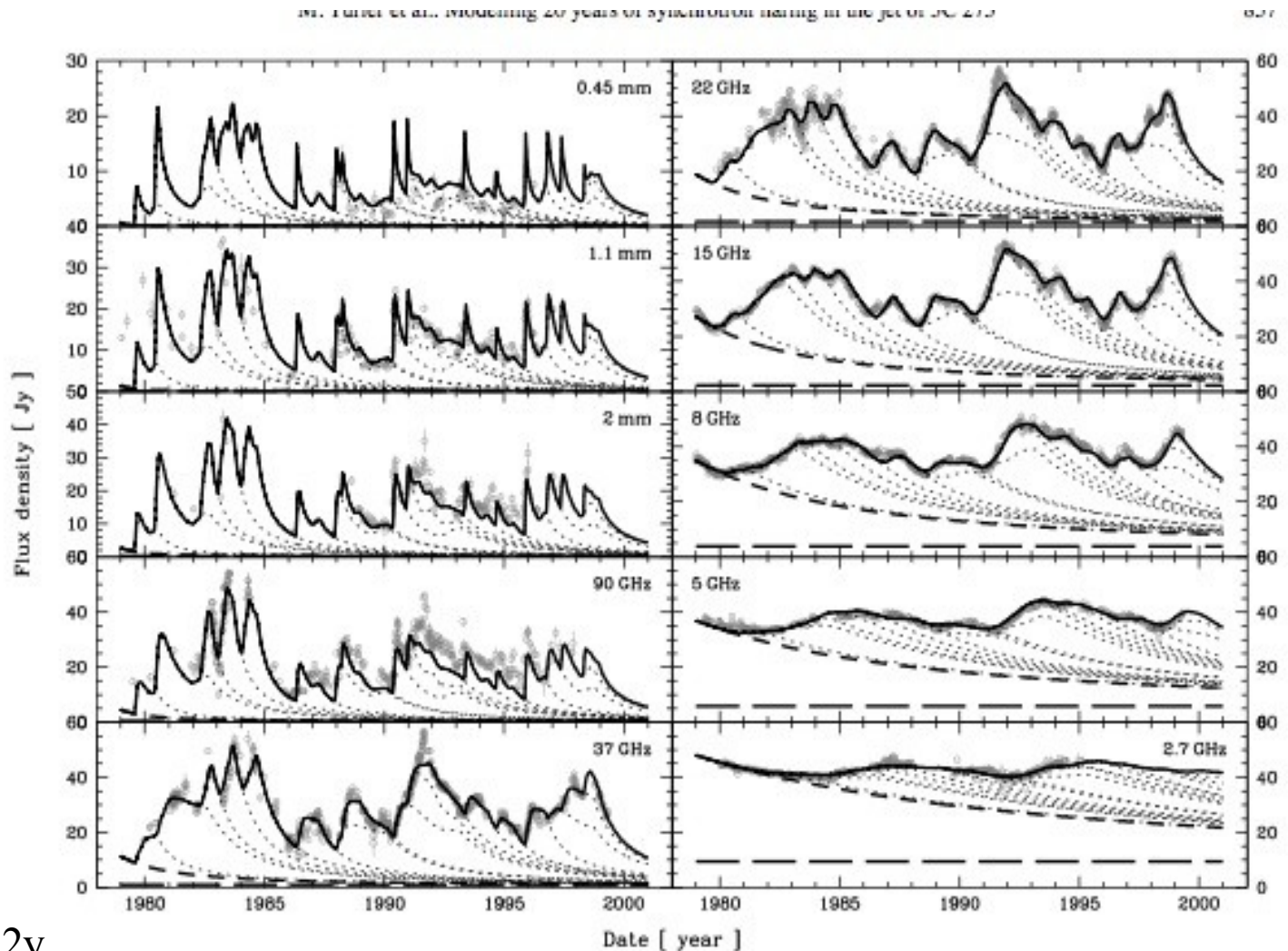
Each flare is described by a “Marsher and Gear” event

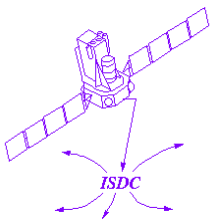
mm to radio light curves and superposed events.

t_0	Knot	t_0 (knot)
1979.6	C5	1978.6 ± 0.04
	C6	1980.0 ± 0.04
1980.9	C6	1980.0 ± 0.04
	X	< 1985.6
1982.4	C7	1982.2 ± 0.4
1983.1	C7a	1983.1 ± 0.00
	C7b	1983.6 ± 0.09
1984.1	C7b	1983.6 ± 0.09
	C8	1984.7 ± 0.10
1986.3	Cx	< 1988.2
1988.1	C9	1988.4 ± 0.17
1990.3	C10	< 1990.2
	D	

Tuerler et al.
2000, 1999

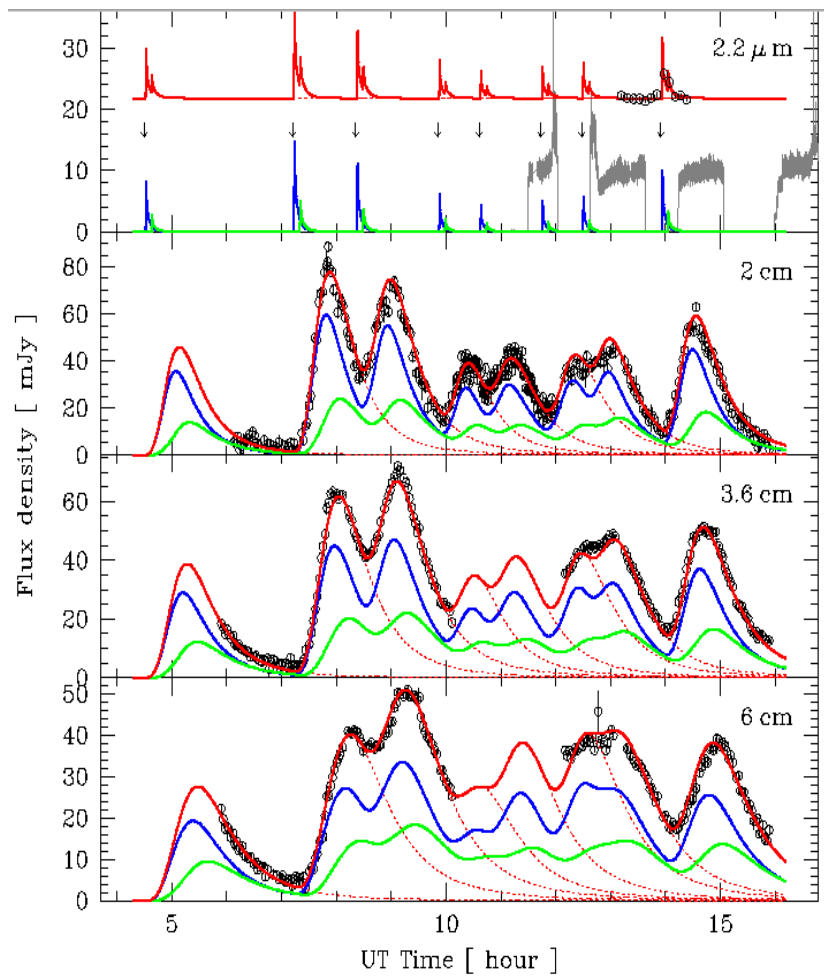
Krichbaum et al. 2000
find correspondence
between ejection
and mm flare within 0.2y



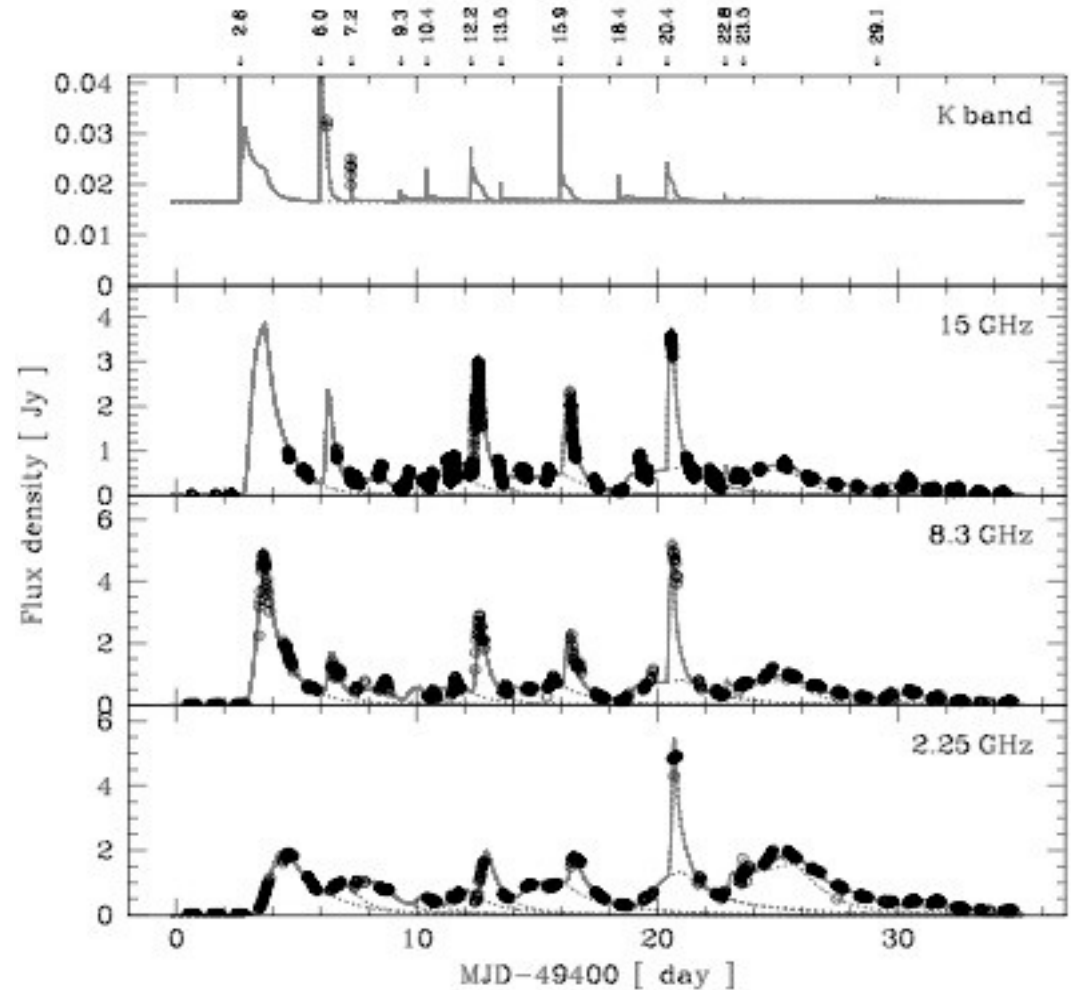


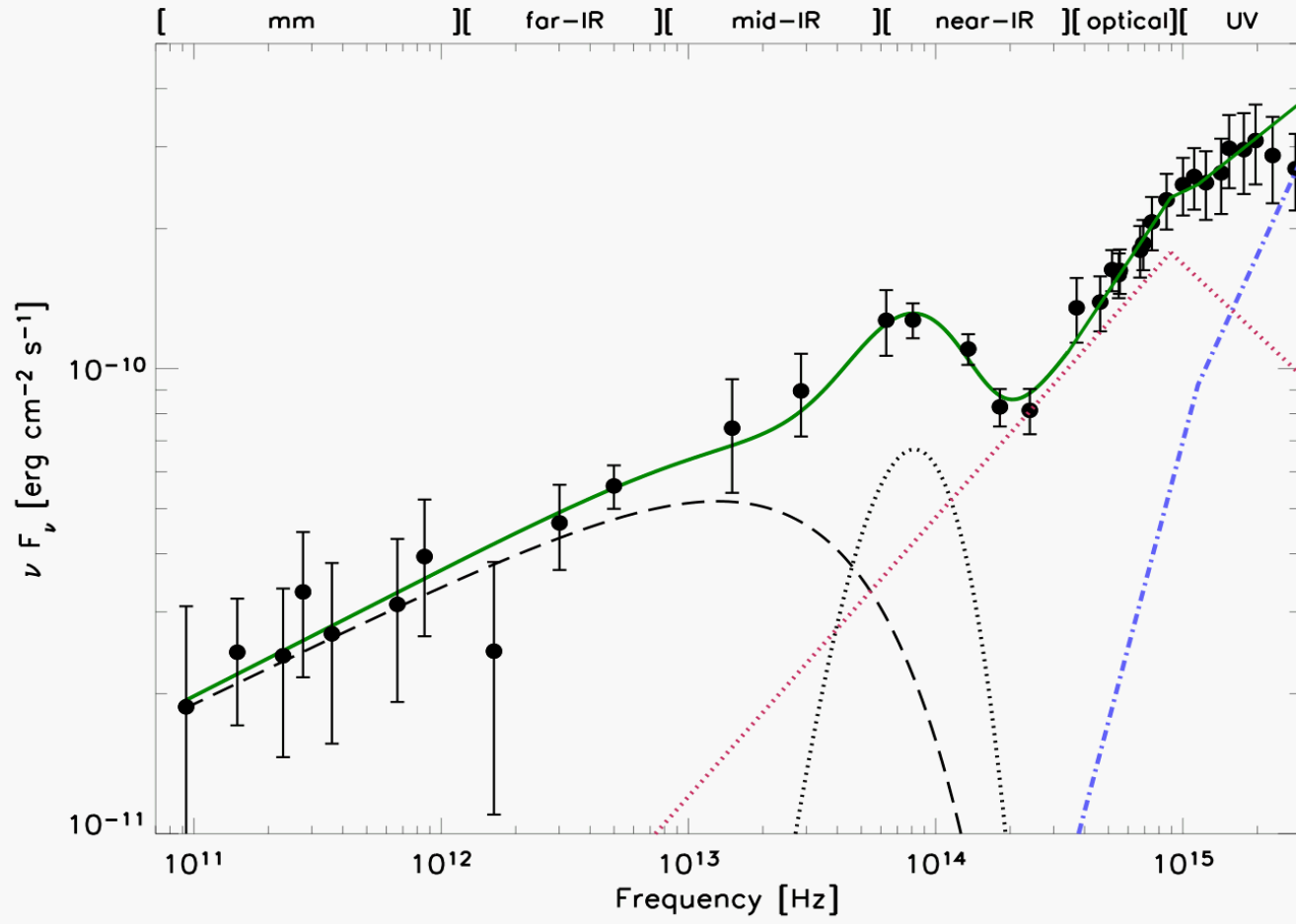
Model successfully extended to micro quasars

1915+105 Tuerler et al 2004



Cyg X-3 Lindfors et al. 2007





Mid IR-IR:
dust emission
range in T

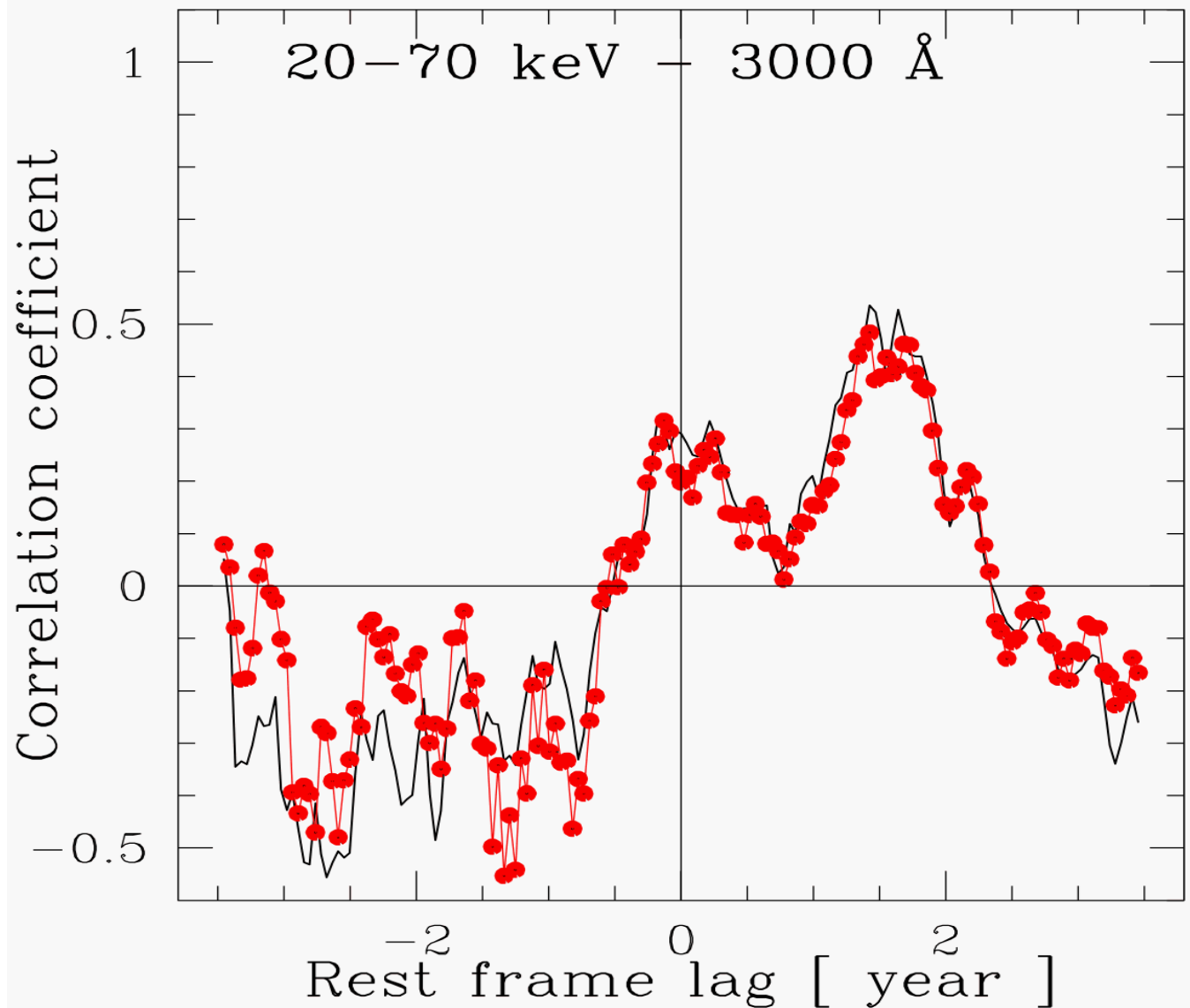
visible-UV:
2 components
(Paltani et al.)
slowly var. R
faster var. B

R: not cont.
emission related
to broad lines.

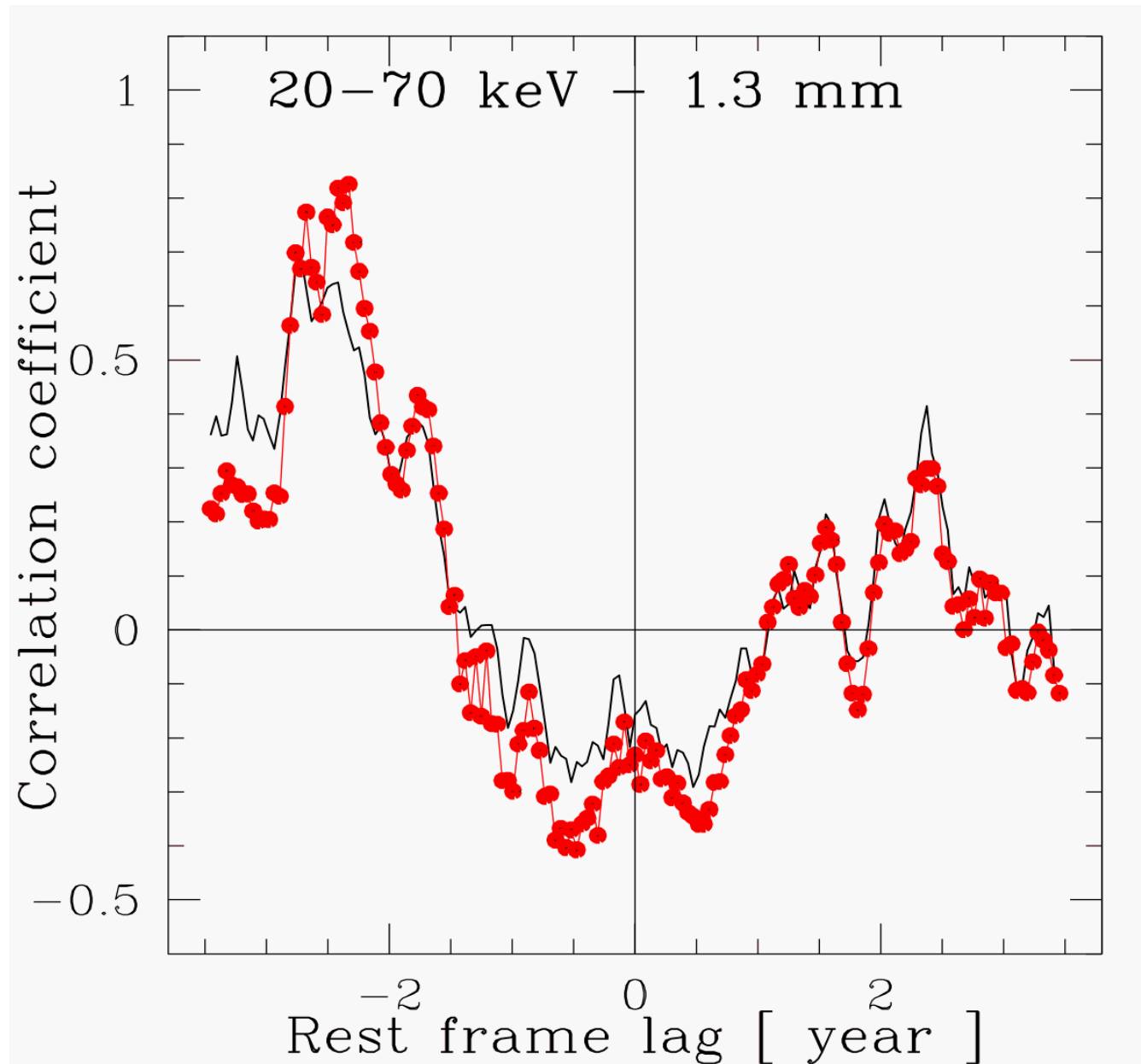
B: associated
with accretion?

No correlation at zero lag between X-rays and B comp.

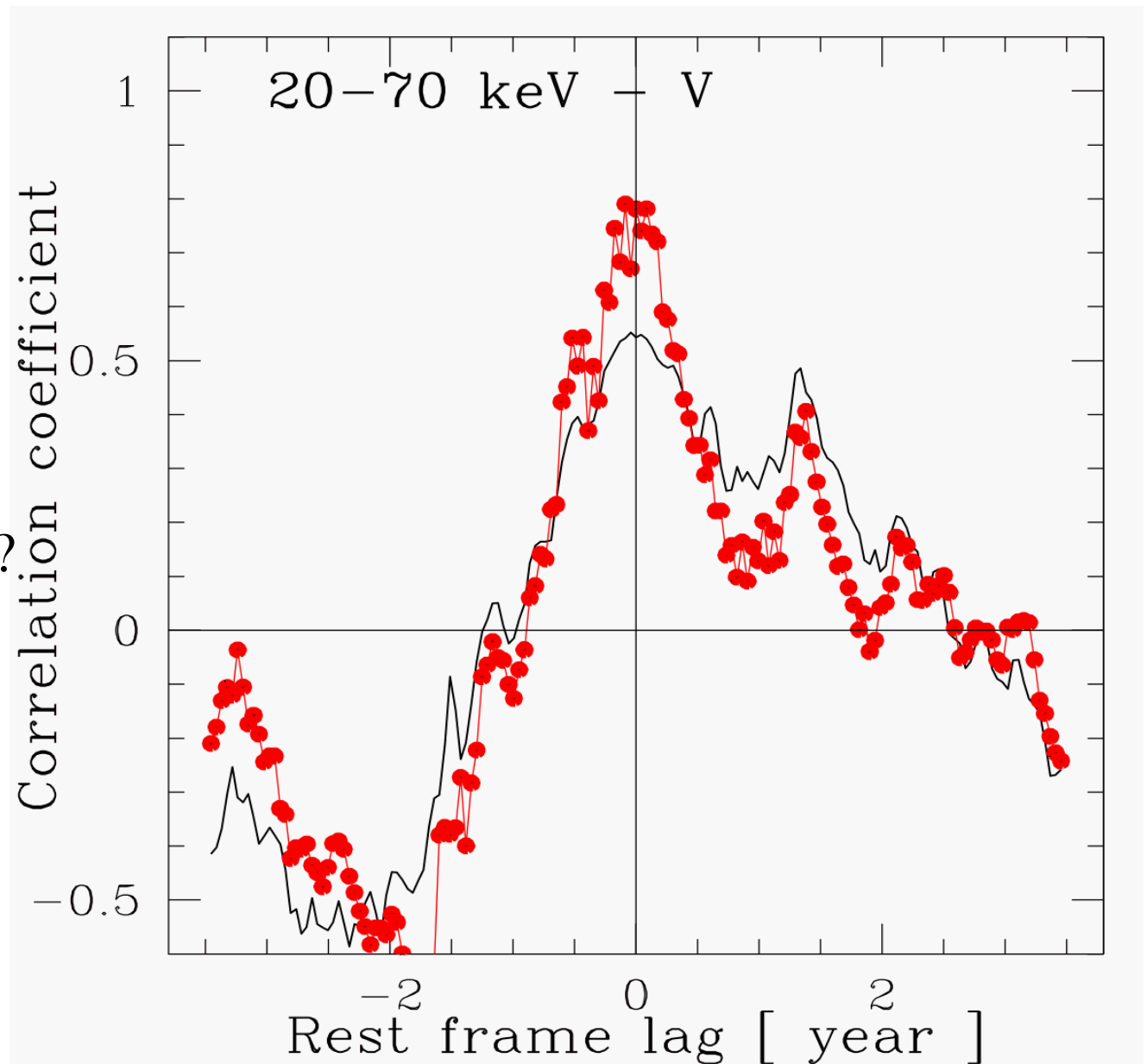
Problem for re-processing needs additional ingredients (parameters)



Hard X-rays
not correlated with
the high energy
synchrotron emission
seen in the jet.



But
hard X-rays
correlate with R
component at short
lags:
same electron population?



Reasonably good understanding of the
radio-mm jet emission

- reproduce light curve
- correlate with birth of VLBI “blobs”

Know that dust is important also in radio loud objects

optical-UV emission is complex, reprocessing?

X-ray emission escapes simple descriptions

spectral index varied over 30 years “secularly” (0.5-0.8)
(Cherniakova et al. 2007)

*why do all components contribute roughly
the same amount to the luminosity?*

Cascades of shocks?

Most AGN models rely on accretion disks

Difficulties of the standard accretion disks to explain observed AGN properties met by working on features of the disk.

Between 1kpc and $100 R_s$ specific angular momentum decreases by $\times 1000$.

Likely to have a “broad” specific angular momentum distribution at $100 R_s$.

Cascades of shocks? (C. and Turler 2005, Ishibashi and C. in prep).

UV light curve well represented by a succession of individual events, variability does not scale as \sqrt{L} . (Paltani et al.)

Alternate model: consider clumps of matter in free fall, interacting with one another at $100 R_s$

Mass of clumps from $V(100R_s)$, energy of individual event (10^{52} ergs).

Shocked clumps form expanding “spheres” that radiate in the UV matter subsequently falls further forming optically thin shocks radiating in the X-rays.

First shock: optically thick, E_{radiated} = fraction of kinetic energy.

$$L_{UV} = \frac{\eta M_c v_{ff}^2}{t_{exp}}$$

$$R_{max} \cong 3 \cdot 10^{15} M_{33}^{1/2} \zeta_{UV}^{-1/4} \text{ cm},$$

$$T \cong 2.6 \cdot 10^4 \eta_{1/3}^{1/4} M_{33}^{-1/8} \zeta_{UV}^{-3/16} \text{ K}.$$

$$\langle L_{UV} \rangle = L_{UV} \cdot \langle N_c \rangle \cong 1.2 \cdot 10^{45} \eta_{1/3} \zeta_{UV}^{-1} \left(\frac{\dot{M}}{10 M_{\odot}/\text{yr}} \right) \text{ erg/s}.$$

T depends on collision parameters, not on M_{BH} . Explains the lack of dependence of the UV spectral shape on luminosity (Walter and Fink 93)

Time evolution of shocks agrees with the short lags observed between light curves.

Result from these first shocks are decentered expanding shells

-lead to outflow on ballistic trajectories

-matter converging: further shocks, optically thin conditions depend on filling factor:

-small mass BH: $R_{\max} \sim 100 R_S$, not for large mass

small mass: Seyfert, large mass: quasars

-shocks: heat ions which heat electrons through Coulomb processes. Electrons cool through Compton processes.

Single electron Compton luminosity

large filling factor (S): (f: fraction of accreted matter in opt. thin shock)

$$L_{Compton} \cong 1.2 \cdot 10^{-12} f_1^{2/7} \eta_{1/3}^{5/7} \zeta_{UV}^{-18/7} E_{p,MeV}^{4/7} \dot{M} M_{BH}^{-2} \text{ erg/s}$$

Low filling factor (Q)

$$L_{Compton} \cong 2.5 \cdot 10^{-13} f_{1/2}^{2/7} \eta_{1/3}^{5/7} \zeta_{UV}^{-18/7} E_{p,MeV}^{4/7} \dot{M} M_{BH}^{-2} \text{ erg/s.}$$

X-ray luminosity: consider electron luminosity,
number of electrons
radiation time

S

$$\langle L_X \rangle \cong 4.8 \cdot 10^{43} f_1^{9/7} \eta_{1/3}^{-2/7} \zeta_{UV}^{-15/14} E_{p,MeV}^{4/7} \dot{M}^2 M_{BH}^{-1} \text{ erg/s}$$

$$\langle L_X \rangle \cong 2.0 \cdot 10^{43} f_1^{9/7} \eta_{1/3}^{-2/7} \zeta_{UV}^{3/7} E_{p,MeV}^{4/7} \dot{M} \text{ erg/s}$$

Q

$$\langle L_X \rangle \cong 1.6 \cdot 10^{43} f_{1/2}^{9/7} \eta_{1/3}^{-2/7} \zeta_X^{15/14} \zeta_{UV}^{-8/7} E_{p,MeV}^{4/7} \dot{M}^2 M_{BH}^{-1} \text{ erg/s}$$

Leads to following L_X/L_{UV} , (A: cooling time longer than free fall)

S: Case A:
$$\frac{\langle L_X \rangle}{\langle L_{UV} \rangle} \cong 0.40 f_1^{9/7} \eta_{1/3}^{-2/7} \zeta_{UV}^{-1/14} E_{p,MeV}^{4/7} M_{BH}^{-1} \dot{M}$$

Case B:
$$\frac{\langle L_X \rangle}{\langle L_{UV} \rangle} \cong 0.17 f_1^{9/7} \eta_{1/3}^{-9/7} \zeta_{UV}^{10/7} E_{p,MeV}^{4/7}$$

Q Case A:
$$\frac{\langle L_X \rangle}{\langle L_{UV} \rangle} \cong 0.01 f_{1/2}^{9/7} \eta_{1/3}^{-2/7} \zeta_X^{15/14} \zeta_{UV}^{-8/7} E_{p,MeV}^{4/7} M_{BH}^{-1} \dot{M}$$

Leads to a range of ratios, with $L_X/L_{UV} < 1$, decreasing with L.

Compared with observations:

Table 2. Observational average $\langle \alpha_{OX} \rangle$ values for the sample and corresponding $\langle L_X/L_{UV} \rangle$ ratios

sample (number of objects)	$\langle \alpha_{OX} \rangle$	$\langle L_X/L_{UV} \rangle$
SDSS main (155)	-1.51 ⁽¹⁾	0.14
high-redshift luminous AGN (36)	-1.72 ⁽¹⁾	0.04
low-redshift Seyfert 1 (37)	-1.34 ⁽¹⁾	0.39
BQS (45)	-1.46 ⁽²⁾	0.19
COMBO (47)	-1.36 ⁽²⁾	0.34
most luminous QSO (33)	-1.80 ⁽³⁾	0.02

⁽¹⁾ Sample from Strateva et al. (2005)

⁽²⁾ Sample from Steffen et al. (2006)

⁽³⁾ Sample from Just et al. (2007)

The observed trend of decreasing UV-X-ray luminosity is well reproduced by the model.

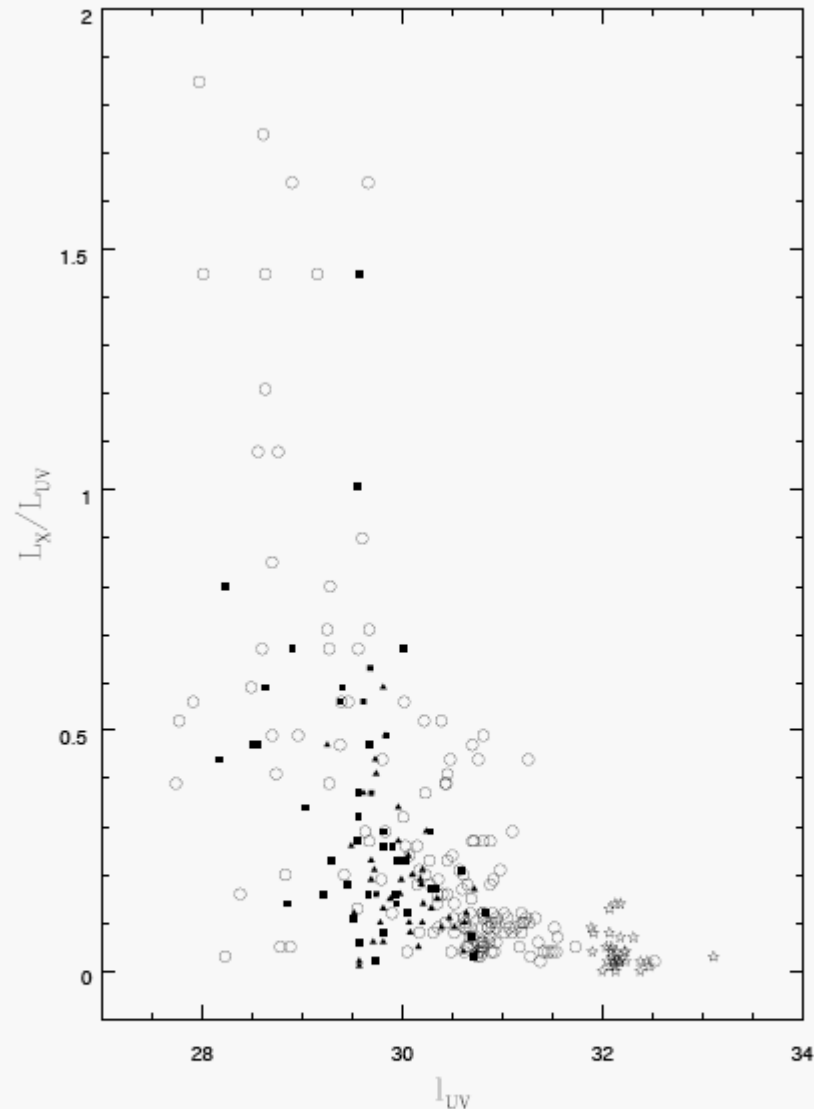


Fig. 1. L_X/L_{UV} versus l_{UV} for the combined sample. The main SDSS sample are represented by open circles, the COMBO sample by filled squares, the BQS sample by filled triangles, and the luminous QSO sample by open stars.

Cascade of shocks model

- relies on a broad angular momentum distribution around 100 Schwarzschild radii
 - provides individual events that explain the UV variability
 - provides “right” temperature for UV emission
 - provides satisfactory understanding of UV lags
 - provides reasonable X-ray to UV luminosity ratios
- Further work will address spectra and variability

At the beginning of the conference

- Detailed description of the centre of our Galaxy
- Good understanding of the jet emission
synchrotron flares
importance of jets in radio loud objects
- Many ingredients for the physics of the accretion
- in BL Lc objects we understand the nature of the X-ray emission
- in QSOs, we have a very poor understanding of
X-ray emission
links between the components